ΠΑΡΑΡΤΗΜΑ Γ

ΜΗ-ΓΡΑΜΜΙΚΗ ΑΝΑΛΥΣΗ ΚΑΙ ΑΣΤΟΧΙΑ ΣΙΔΗΡΩΝ ΚΑΜΠΥΛΩΝ ΣΩΛΗΝΩΝ ΥΠΟ ΚΑΜΨΗ ΚΑΙ ΠΙΕΣΗ

Στο παράρτημα αυτό παρατίθεται η κάτωθι εργασία η οποία υποβλήθηκε για δημοσίευση στο περιοδικό *Journal of Pressure Vessel Technology*, της Αμερικανικής Ένωσης Μηχανολόγων Μηχανικών, ASME, και αναφέρεται στην αντοχή ελαστοπλαστικών σωληνωτών τμημάτων (elbows).

[1] Karamanos, S. A., Giakoumatos, E. and Gresnigt, A. M., "Nonlinear Response and Failure of Steel Elbows under In-plane Bending and Pressure.", *Journal of Pressure Vessel Technology*, ASME, submitted for publication, November 2002.

Η εργασία έγινε σε συνεργασία με το Τεχνικό Πανεπιστήμιο του Delft, Ολλανδία, Τμήμα Πολιτικών Μηχανικών.

Η εργασία εξετάζει την απόκριση καμπύλων σωλήνων υπό κάμψη στο επίπεδό τους και υπό πίεση, χρησιμοποιώντας μία αριθμητική μέθοδο πεπερασμένων στοιχείων, και υποστηριζόμενη από πειραματικά δεδομένα. Η αριθμητική διερεύνηση βασίζεται σε ένα ειδικό στοιχείο «σωλήνα», το οποίο μπορεί να περιγράψει την παραμόρφωση του σωλήνα με εύρωστο τρόπο, λαμβάνοντας υπόψη γεωμετρικές μη-γραμμικότητες και ανελαστική συμπεριφορά. Επιπλέον χρησιμοποιείται ένα μη-γραμμικό ανελαστικό πεπερασμένο στοιχείο κελύφους από ένα γενικό πρόγραμμα πεπερασμένων στοιχείων. Παρουσιάζονται αριθμητικά αποτελέσματα για σχετικώς λεπτότοιχους σωλήνες και εξετάζεται η επιρροή των γειτονικών ευθύγραμμων μελών. Τα αριθμητικά αποτελέσματα συγκρίνονται επιτυχώς με πειραματικά αποτελέσματα, και έτσι εξετάζονται ορισμένα ειδικά θέματα της συμπεριφοράς των σωλήνων. Η επιτυχής σύγκριση των αριθμητικών αποτελεσμάτων με τα πειράματα αφορά τον δρόμο ισορροπίας ροπής-καμπυλότητας, την παραμόρφωση της κρίσιμης διατομής καθώς και την δημιουργία τοπικής αστοχίας (ήβωσης). Τέλος, χρησιμοποιώντας τα αριθμητικά εργαλεία, εξετάζεται η αστοχία των σωλήνων υπό κάμψη λόγω «οβαλοποίησης» της διατομής ή λόγω τοπικό λυγισμό, κάνοντας άμεση αναφορά στις παραμορφώσεις των δοκιμίων των πειραμάτων.

NONLINEAR RESPONSE AND FAILURE OF STEEL ELBOWS UNDER IN-PLANE BENDING AND PRESSURE

S. A. Karamanos[1], *E. Giakoumatos*
Department of Mechanical and Industrial Engineering
University of Thessaly, Volos 38334, Greece

A. M. Gresnigt
Faculty of Civil Engineering and Geosciences
Delft University of Technology, Delft 2600 GA, The Netherlands

ABSTRACT

The paper investigates the response of elbows under in-plane bending and pressure, through a finite element formulation, supported by experimental results from real-scale tests. The finite element technique is mainly based on a nonlinear three-node "tube element", capable of describing elbow deformation in a rigorous manner, and considers geometric and material nonlinearities. Furthermore, a nonlinear shell element from a general-purpose finite element program is employed in some special cases. Numerical results are compared with experimental data from steel elbow specimens. The comparison allows the investigation of some important issues regarding deformation and moment capacity of elbows. Results from relative-thin elbows show the effects of pressure and the influence of straight pipe segments. Finally, using the numerical tools, failure of elbows under bending moments is examined (cross-sectional flattening or local buckling), and reference to experimental observations is made.

1 INTRODUCTION

Curved pipe segments (elbows) are widely used in industrial piping and pipelines. Because of their ability to sustain significant deformations, elbows can accommodate thermal expansions and absorb other externally-induced loads (e.g. seismic ground motions). Following the pioneering work of Von Karman [1], several researchers worked on elbow flexibility and stress intensity, and reported analytical solutions, supported by experimental evidence, for in-plane and out-of-plane bending under internal pressure [2], [3], [4], [5]. The above works have constituted the basis of current elbow stress design rules (e.g. [6]).

The development of computational methods (e.g. finite elements), enabled the numerical investigation of elbow response. Marcal [7], combining curved-beam theory and toroid shell theory, proposed a finite element

[1] Corresponding author. Tel. +30 24210 74086, FAX +30 24210 74012, email: skara@mie.uth.gr

for pipe stress analysis. Sobel [8] studied the linear bending response of elastic elbows comparing previous analytical results using two computer programs (ELBOW and MARC), and presented results for flexibility and stress intensity factors. Based on thin-shell kinematics, Ohtsubo and Watanabe [9] developed "ring elements" for the stress analysis of pipe bends. In more recent publications, several special-purpose "pipe" or "elbow" elements were developed, which combine cross-sectional deformation with longitudinal beam deformation [10], [11], [12], [13]. Some of those elements are incorporated in general-purpose finite element commercial software packages (e.g. MARC, ABAQUS, ADINA).

In a series of tests on 16-inch 90° elbows, Sobel and Newman [14], [15], and Dhalla [16] investigated the ultimate capacity of elbows (D/t=39 and R/r=3) under closing moments and reported variations of stress and strain around the elbow cross-section and along the pipe. The experimental results were compared with numerical results from shell elements and simplified elbow elements. Gresnigt et al. [17] reported test results on 30° and 60° elbows (R/r=6) under in-plane bending and pressure, and reported moment-curvature curves, variations of ovalization along the length, and pressure effects on elbow flexibility. Those tests are examined in detail in the present paper, and compared with numerical results. Hilsenkopf et al. [18] reported experimental results on thin-walled (D/t=89.5) stainless steel elbows and thick-walled (D/t=13.4) ferritic elbows under in-plane and out-of-plane bending, in connection with their functional capability. Effects of pressure, temperature, cyclic loading and secondary stresses were also investigated. Suzuki and Nasu [19] conducted two closing moment tests on 12-inch (D/t=46.3) and 24-inch (D/t=64.9) elbows. The response was compared with numerical predictions from four-node shell elements. In a recent paper, Tan et al. [20] performed one closing and one opening moment test on 90° thick stainless steel elbows (D/t=10.5). The results were compared with shell and elbow element results.

In the above works, cross-sectional deformation (ovalization) has been recognized as a very important issue for elbow bending behavior. In particular, the ultimate bending capacity of elbows is associated with strains far beyond the elastic limit, as well as with significant distortion of pipe cross-section. To model elbow response at the ultimate condition, a nonlinear analysis accounting for both material and geometric nonlinearities is required. Gresnigt and Van Foeken [21], [22] presented an analytical formulation for the elastic-plastic cross-sectional deformation of elbows, introducing a correction factor to take into account the influence of the adjacent straight pipe segments. Their results were in fairly good agreement with experiments. Using element ELBOW31B of ABAQUS, Shaleby and Younan [23], [24] analyzed steel elbow segments

(R/r=3) for a wide range of diameter-to-thickness ratios ($15.5 \leq D/t \leq 97$), under in-plane bending (opening and closing moments) and internal pressure, assuming constant curvature along the elbow. Chattopadhyay et al. [25] have employed general-purpose program NISA to analyze thick steel 90° elbows ($D/t<25$), through twenty-node fully-integrated solid elements and, using a curve-fitting procedure, they proposed simplified formulae for the collapse (limit) moment capacity in terms of pressure and the bend factor $h=tR/r^2$.

The present paper is aimed at investigating some special issues of elbow response under the simultaneous action of in-plane bending and pressure. Emphasis is given on the ultimate capacity and failure of relatively thin pipes. A nonlinear finite element formulation, which takes into account geometrical and material nonlinearities in a rigorous manner, is employed. Results from real-scale elbow tests [17] are compared with the predictions from the numerical formulation, in terms of elbow flexibility and ultimate capacity. Finally, based on experimental observations and numerical predictions the failure (collapse) of thin-walled elbows due to excessive cross-sectional ovalization or local buckling is discussed.

2 NONLINEAR FINITE ELEMENT TECHNIQUE

A nonlinear finite element formulation, developed elsewhere [26], [27], is employed accounting for material and geometric nonlinearities. The constitutive model accounts for inelastic effects through a large-strain J_2-plasticity model, with isotropic hardening, considering the condition of zero normal stress in the radial tube direction. To trace nonlinear unstable post-buckling equilibrium paths, a path-follower (arc-length) algorithm is implemented.

The main feature of the formulation is the "tube element", a special-purpose element for the analysis of pipes and pipelines, which combines longitudinal (beam-type) deformation with cross-sectional deformation. The formulation is based on a Lagrangian description with convected coordinates in the hoop, longitudinal and radial direction (denoted as θ, ζ, ρ respectively). The isoparametric beam element concept is used to describe longitudinal deformation, with three nodes along the tube element axis (Figure 1a). Bending is applied about a fixed Cartesian axis x_1 so that x_2-x_3 is the plane of bending, and each node possesses three DOFs (two translational along x_2 and x_3 and one rotational about x_1).

To describe cross-sectional deformation, thickness is assumed to be constant and a reference line is chosen within the cross-section. The kinematic relations follow ring theory [28], and are appropriately enhanced to account for out-of-plane deformation. The position of the reference line with respect to node (k) is

$$\mathbf{r}^{(k)}(\theta) = x_r(\theta)\,\mathbf{e}_x^{(k)} + y_r(\theta)\,\mathbf{e}_y^{(k)} + z_r(\theta)\,\mathbf{e}_z^{(k)} \tag{1}$$

where the orthonormal vectors $\mathbf{e}_x^{(k)}, \mathbf{e}_y^{(k)}, \mathbf{e}_z^{(k)}$ define cross-section orientation, and

$$\begin{aligned} x_r(\theta) &= \left[r + w(\theta)\right]\cos\theta - v(\theta)\sin\theta \\ y_r(\theta) &= \left[r + w(\theta)\right]\sin\theta + v(\theta)\cos\theta \\ z_r(\theta) &= u(\theta) \end{aligned} \tag{2}$$

are the components of $\mathbf{r}^{(k)}(\theta)$ with respect to the cross-section vector triplet, and $w(\theta)$, $v(\theta)$ and $u(\theta)$ are displacements of the reference line in the radial, tangential and out-of-plane (axial) direction respectively (Figure 1). Material fibers in the radial direction can rotate in the out-of-plane direction by $\gamma(\theta)$ and the position vector of an arbitrary point in the deformed configuration is

$$\mathbf{x}(\theta,\zeta,\rho) = \sum_{k=1}^{3}\left[\left(\mathbf{x}^{(k)} + \mathbf{r}^{(k)}(\theta) + \rho\mathbf{n}^{(k)}(\theta) + \rho\gamma(\theta)\mathbf{e}_z^{(k)}\right)N^{(k)}(\zeta)\right] \tag{3}$$

where $\mathbf{x}^{(k)}$ is the position vector of node (k), $N^{(k)}(\zeta)$ is the corresponding quadratic interpolation polynomial, and $\mathbf{n}^{(k)}(\theta)$ is the "in-plane" outward normal of the reference line. Functions $w(\theta)$, $v(\theta)$, $u(\theta)$ and $\gamma(\theta)$ are discretized as follows, considering symmetry with respect to the x_2-x_3 plane ($\theta = \pm\,\pi/2$):

$$\begin{aligned} w(\theta) &= a_0 + a_1\sin\theta + \sum_{n=2,4,6,\ldots} a_n\cos n\theta + \sum_{n=3,5,7,\ldots} a_n\sin n\theta \\ v(\theta) &= -a_1\sin\theta + \sum_{n=2,4,6,\ldots} b_n\sin n\theta + \sum_{n=3,5,7,\ldots} b_n\cos n\theta \\ u(\theta) &= \sum_{n=2,4,6,\ldots} c_n\cos n\theta + \sum_{n=3,5,7,\ldots} c_n\sin n\theta \\ \gamma(\theta) &= \gamma_0 + \gamma_1\sin\theta + \sum_{n=2,4,6,\ldots} \gamma_n\cos n\theta + \sum_{n=3,5,7,\ldots} \gamma_n\sin n\theta \end{aligned} \tag{4}$$

where a_n, b_n are the "ovalization" parameters and c_n, γ_n are the "warping" parameters.

The element formulation is capable of considering expansions of $w(\theta)$, $v(\theta)$, $u(\theta)$ and $\gamma(\theta)$ up to any degree. For the purposes of the present work, expansions up to the 16th degree [$n \le 16$ in equations (8)] are employed. Regarding the number of integration (Gauss) points in the hoop direction, a short parametric study [29] indicated that the 16th degree expansion requires 19 equally-spaced integration points around the half-

circumference including the two points on the symmetry plane. Five and two Gauss points are used in the radial (through the thickness) direction and the longitudinal direction respectively.

The above "tube element" formulation is implemented in a special-purpose (in-house) finite element program, which has been verified conducting comparisons with results from analytical solutions, isoparametric shell elements, and experimental data [25], [26], [29], [30].

In addition to the above "tube element" technique, the general-purpose commercial program ABAQUS [13] is also employed. The program has excellent graphical capabilities for presenting the results, and an extensive library for shell and elbow elements. In particular, shell element S8R5 is employed for more detailed simulation and analysis of some special cases. Moreover, elbow element ELBOW32 is used for comparison purposes. This elbow element has several similarities with the above-described tube element, but considers Fourier expansion up to the 6^{th} degree only. Nonlinear geometry is considered and inelastic effects are accounted for through a J_2 large strain plasticity model with isotropic hardening. A path-follower (Riks) algorithm is employed to trace unstable equilibrium paths. Comparisons between the present "tube element" formulation and the ABAQUS shell or elbow elements are reported in the present paper for some specific cases.

3 TNO ELBOW EXPERIMENTS

A series of real-scale steel elbow tests, conducted at TNO [17], were aimed at examining the response of short-bend-radius (R/r=6) elbows under in-plane bending (opening and closing end moments) and pressure. The test specimens consisted of six moderately thin walled elbows (∅ 160 – 2.9 mm, D/t=55) and four thin walled elbows (∅ 261 – 2.9 mm, D/t=90). Each specimen consisted of two straight parts, and a curved part, corresponding to an angle of 30° or 60° (Figure 2). Specimen parameters are presented in Table 1. The yield stress of the material (σ_y) is equal to 380 MPa, and a negligibly low hardening modulus E′ has been measured.

The experimental set-up is shown in Figure 3. Bending action was produced by means of the two hydraulic cylinders on the left and right respectively, which produce a four-point bending. The change in cross-sectional rotation was measured through the displacement transducers mounted in the steel frames, welded to the pipe bend. The change in the vertical diameter was measured with the dial gauges in the stirrup-type measuring devices.

First, each specimen was tested in the elastic range under in-plane bending in the presence of several internal pressure levels, to examine the effects of pressure on elbow flexibility. Subsequently, the elbows were bent until collapse. Eight specimens were tested under in-plane bending only (without internal pressure), and two specimens (Nos. 74 and 75) were tested under in-plane bending in the presence of internal pressure equal to about 60% of the fully-plastic pressure ($p_y=2\sigma_y t/D_m$, where D_m is the mean tube diameter). For each elbow configuration, both closing and opening bending moments were considered (Table 1). Tests results are reported in Section 4, together with finite element predictions.

Figure 3 shows specimen No. 75 at the end of the test. Note that deformations occurred mainly in the elbow area, whereas the straight parts were significantly less deformed. Figure 4, shows the final collapsed shapes of thin-walled specimens 82, 83 and 84 at the middle section.

Specimen No.	D (mm)	t (mm)	R (mm)	Angle α	Pressure (MPa)	Bending type
70	160	2.9	480	30°	0	closing
71	160	2.9	480	30°	0	opening
72	160	2.9	480	60°	0	closing
73	160	2.9	480	60°	0	opening
74	160	2.9	480	30°	8.77	closing
75	160	2.9	480	30°	8.77	opening
81	261	2.9	772	30°	0	closing
82	261	2.9	772	30°	0	opening
83	261	2.9	772	60°	0	closing
84	261	2.9	772	60°	0	opening

Table 1: Elbow specimens tested at TNO [17]

4 NUMERICAL RESULTS AND COMPARISON WITH TEST DATA

Using the aforementioned numerical tools, a cross-sectional (ovalization) analysis is conducted first to examine the effects of pressure on cross-sectional capacity and ovalization. Subsequently, the TNO experiments [17] are simulated and, finally, failure of thin-walled elbows is investigated and discussed.

4.1 Cross-sectional elbow response

Figure 5 shows the cross-sectional response of a thin walled curved pipe for three levels of internal pressure under closing and opening bending. The bending moment is assumed constant along the pipe, and the

pipe is infinitely long, free of boundary conditions. Thus, all cross-sections exhibit the same deformation without warping and a two-dimensional analysis is conducted with only one element in the longitudinal direction, restraining all warping degrees of freedom ($c_n=\gamma_n=0$). The cross-sectional and material properties of the pipe are those of specimens 81 – 84 (D=261 mm, t=2.9 mm, R/r=6, E=210 GPa, σ_y=380 MPa and a zero post-yield modulus up to 2% strain). The values of moment M, curvature k and pressure p are normalized by the fully plastic moment $M_p=\sigma_y D_m^2\, t$, the curvature-like parameter $k_I=t/D_m^2$ and the fully plastic pressure p_y respectively ($m=M/M_p$, $\kappa=k/k_I$).

The ovalization of elbow cross-section is expressed in terms of the ovalization parameter:

$$ov=\frac{D'_h - D'_v}{2D_m} \qquad (5)$$

where D'_h and D'_v are the deformed lengths of the horizontal diameter (normal to the plane of bending) and of the vertical diameter (on the plane of bending). The ovalization parameter is shown in Figure 6, in terms of the applied curvature. When closing moments are applied, "positive" ovalization occurs, with shortening of the vertical diameter. This reduces the moment capacity of the cross-section, and the ultimate moment is significantly low, especially for zero pressure (less than 20% of M_p). The presence of pressure decreases ovalization and causes an increase of the ultimate moment.

On the other hand, opening moments result in "negative" ovalization (extension of the diameter on the plane of bending). This mechanism increases the moment capacity of the pipe cross-section and enables the pipe to sustain significantly larger moments than the corresponding moments under closing bending. This significant difference between closing and opening moment capacity has also been noted in previous publications [21], [22], [23], [24], [25].

4.2 Comparison with TNO elbow test data

Figures 7, 8 show the moment-rotation curves obtained from the experiments, compared with the "tube" element results, for specimens 81, 82, 83 and 84. Bending moment is plotted in terms of the relative rotation φ_{CE} between cross-sections C and E, the ends of the curved pipe segment (Figure 2). Due to symmetry with respect to the middle section, $\varphi_{CE}=2\varphi_C$. It is important to note that the rotation of a cross-section is defined differently in experiments and in analysis. Experimentally, it is measured through the rotation of the steel

frames attached to the elbow at the mid-height of the cross-section (Figures 3, 4). In tube element analysis, the rotation of a cross-section is determined from the value of the rotational DOF of the corresponding node of the tube element. To investigate further this issue, these four specimens are also analyzed with shell element S8R5 of ABAQUS, and the rotation of cross-section C is calculated from the relative displacements of two shell nodes on this cross-section. When the top and bottom nodes of the cross-section are employed to calculate the rotation (namely points CT and CB in Figure 9), then the corresponding initial stiffness is very close to the stiffness obtained from tube element analysis. However, when two nodes very close to the cross-section mid-height are employed to calculate the rotation (namely points CM1 and CM2 in Figure 9), the calculated stiffness becomes similar to the experimental value. Cross-sectional warping constitutes the main reason for this difference, and it is due to the influence of the adjacent straight pipe segments. Note that specimens 81 and 82 have a small curved part (L_c=1.6D), so that the pipe cross-section exhibits significant warping at C. This effect is alleviated in specimens 83 and 84, because the curved pipe portion is significantly longer (L_c=3.1D). In other words, section C of specimens 83 and 84, exhibits less warping deformation and this accounts for the fairly good comparison between experimental and numerical values of initial stiffness, shown in Figures 7, 8. The above results also indicate that rotation measurements at the mid-height points (used in experiments) may not be representative for the average cross-sectional rotation.

Figures 10, 11 and 12 show the comparison of the experimental moment-rotation (M-φ_{CE}) curves with the corresponding numerical results for specimens 70, 71, 72, 73, 74 and 75. Note that results from ELBOW32 element are practically identical to tube element results when a 6th degree Fourier expansion is employed. The results in those Figures verify that the ultimate capacity under opening moments is significantly higher than the ultimate capacity under closing moments. In addition, under closing moments, pressurized elbows (specimen 74) are capable of sustaining larger bending moments than non-pressurized pipes (specimens 70, 72), due to the "stiffening" effect of pressure, which decreases cross-sectional ovalization.

In Figure 10, tube element analysis appears to underestimate the initial stiffness of specimens 70, 71, and this is attributed to the small value of the elbow angle (30°), as discussed in detail in a previous paragraph for specimens 81 and 82. On the other hand, the initial stiffness predicted by the tube element is improved in specimens 72, 73 (Figure 11), because of the larger value of elbow angle (60°). Furthermore, Figure 12 shows a very good comparison between tube element analysis and test data for pressurized specimens 74, 75.

Another interesting observation concerns the ultimate moment of the elbows under closing moments. In Figures 7, 8 numerical results show that there exists a considerable difference on the maximum moment of specimens 81 and 83 (22,200 N-m versus 16,400 N-m). Similar values are obtained experimentally. Furthermore, those moments are significantly higher than the ultimate moment obtained from cross-sectional analysis, as shown in Figure 5 (12,900 N-m). The above differences are due to the length of the curved pipe segments L_c. In specimen 81, the curved portion of the pipe is short (L_c=1.6D). Thus, a higher moment capacity is obtained in specimen 81 than in specimen 83 (L_c=3.1D), due to the strong influence of the adjacent straight pipe segment. Furthermore, the two-dimensional analysis (Figure 5) corresponds to an infinite length of the curved portion (L_c=∞) and this accounts for the smallest ultimate moment.

Figure 13 shows the influence of pressure on the initial flexibility of thin-walled specimens 83 and 84. Experimental and numerical results from tube element analysis verify the well-known stiffening effect of internal pressure on elbow flexibility, and a very good comparison between experiments and analysis is obtained. Finally, in Figure 14, cross-sectional flattening at the middle cross-section is plotted in terms of rotation φ_{CE}, for specimens 83 and 84. Flattening is measured in terms of ΔD, which is the shortening (specimen 83) or lengthening (specimen 84) of the diameter on the plane of bending. In both specimens very good agreement between numerical results and test data is obtained.

4.3 Failure of thin-walled elbows

After the onset of plastic deformation, the elbow is capable of sustaining further deformation, without loss of strength. However, at some stage, the pipe fails, in the sense that significant local deformations occur because of excessive cross-sectional ovalization or local buckling. In the following, failure of thin-walled elbows is examined.

Experimental observations and numerical results indicate that, under closing moments, the response of an elbow results in "limit moment" instability and the elbow fails due to excessive cross-sectional flattening in the form of a four-equally-spaced-plastic-hinge mechanism, as shown Figure 15a for specimen 83. This configuration is consistent with the corresponding shape of the specimen, shown in Figure 4a, as well as with analytical results presented in [21], [22] for short-radius pipe elbows.

An entirely different response is observed under opening moments (specimens 82 and 84). The response is significantly stiffer than in the case of closing moments (specimen 83). Moreover, those elbows exhibit local buckling at the "outer" side of the pipe cross-section. This is observed in experiments (Figure 4b, 4c), and verified by the numerical results (Figure 15b - specimen 84).

It is possible to use a simple (heuristic) argument to verify the location of buckles around the pipe cross-section, considering the pre-buckling distorted (ovalized) cross-sectional configuration. This simple argument was first proposed and verified numerically in [34] for the case of elastic thin cylinders initial straight with non-deformed cross-section subjected to bending. Subsequently, Axelrad [35] employed this argument for analysing bifurcation of elastic tubes under bending, taking into account cross-sectional ovalization. A finite element verification of Axerlad's hypothesis was recently presented in [30]. Herein, we extend this argument for inelastic tube bending. The argument is based on the buckling stress formula for cylindrical shells under uniform compressive stress σ_u in the longitudinal direction:

$$\sigma_{u,cr} = \eta C E\left(\frac{t}{r}\right) \tag{6}$$

where C is a factor accounting for initial imperfections [32], and η ($0<\eta\leq 1$) is a plasticity reduction factor, which depends on the stress level [33]. If C=0.605 and η=1, then equation (6) reduces to the classical formula for elastic buckling of thin cylindrical metal shells [28]. In the case of tubes subjected to bending, longitudinal stresses are no longer uniform around the cross-section and the cross-section is not circular because of ovalization. Therefore, equation (6) cannot be applied directly. However, it can still be employed in a local sense; it is assumed that the cross-section buckles at the location where the local compressive longitudinal stress reaches a value equal to

$$\sigma'_{u,cr} = \eta C E\left(\frac{t}{r'}\right) \tag{7}$$

where $1/r'$ is the local hoop curvature of tube wall at a specific location around the circumference, calculated as follows [28]:

$$\frac{1}{r'} = \frac{1}{r} + \frac{1}{r^2}\left(v' - w''\right) \tag{8}$$

The location around the cross-section at which longitudinal stress reaches first a value equal to the buckling resistance $\sigma'_{u,cr}$ [equation (7)] is considered to be the "critical location" of the cross-section at which buckling occurs.

In elbows under opening moments, "negative" ovalization occurs, so that at points located on the "outer" side of the cross-section the pipe wall is nearly flat, corresponding to a very small value of local curvature $1/r'$ (Figures 15b and 16a). Therefore, according to equation (7), a small value of buckling resistance is expected at those points. Furthermore, the variation of longitudinal stresses at the middle cross-section of specimen 84 at the buckling stage, as obtained from FE analysis (Figure 16b), indicates that significant inelastic compressive stresses occur in the area where $-60^\circ \leq \theta \leq 0^\circ$, which is actually the area that buckling occurs. The above considerations explain the location and the shape of the buckles obtained experimentally and numerically.

5 CONCLUSIONS

Using nonlinear finite element tools, supported by experimental evidence, the response of relatively thin steel elbows under in-plane bending and pressure is examined (D/t=55, D/t=90). A special-purpose finite element formulation, which employs a nonlinear "tube element", is mainly employed. Furthermore, in some specific cases, results from a general-purpose finite element program are also obtained.

Cross-sectional finite element analysis of thin-walled curved pipes indicates that internal pressure has an important effect on both ultimate moment and cross-sectional ovalization, and a significant difference between closing and opening moment response is observed, also noted in previous works.

Results from the nonlinear finite element analysis are compared with experimental data from 30° and 60° steel elbows. Good comparison is obtained in terms of elbow flexibility, including pressure effects. Furthermore, the experimental moment-rotation curves are successfully compared with the corresponding curves from the finite element results. Both experimental data and analytical results verify the significantly different response for closing moments and for opening moments, as well as the reduction of cross-sectional deformation due to internal pressure. It is also concluded that the adjacent straight parts of the pipe have a considerable influence on the response and the ultimate moment of the elbow.

Based on experimental observations and numerical results, the present paper also investigates failure of thin-walled elbows under in-plane bending. A different failure mode is detected for closing bending and for

opening bending conditions. Elbows under closing bending moments fail because of significant cross-sectional deformation (ovalization), whereas elbows under opening bending moments exhibit local buckles at the "outer" side of the pipe cross-section. Finally, a heuristic argument is employed to explain the location of the buckles and the shape of the post-buckled cross-section under opening bending moments.

ACKNOWLEDGMENTS

This work has been partially supported by the Earthquake Planning & Protection Organization (EPPO), Athens, Greece.

REFERENCES

[1] Karman, Th. von, 1911. "Uber die Formuanderung dunnwandiger Rohre" [in German], *Zeit. Des Vereines deutcher Ingenieure*, Vol. 55, pp. 1889-1895.

[2] Pardue, T.E. and Vigness J., 1951. "Properties of Thin-Walled Curved Tubes of Short-Bend Radius", *Transactions of the ASME*, Vol. 73, pp. 77-87.

[3] Gross, N., 1952. "Experiments on Short-radius Pipe-bends", *Proceedings of the Institution of Mechanical Engineers* (B), Vol. 1B, pp. 465-479.

[4] Gross, N. and Ford, H., 1952. "The Flexibility of Short-radius Pipe-bends", *Proceedings of the Institution of Mechanical Engineers* (B), Vol. 1B, pp. 480-491.

[5] Rodabaugh, E. C., and George, H. H., 1957. "Effect of internal pressure on the flexibility and stress intensification factors of curved pipe or welding elbows", *Transactions of the ASME*, Vol. 79, pp. 939-948.

[6] American Society of Mechanical Engineers, 1993, *Chemical Plant and Petroleum Refinery Piping*, ASME 31.3, 1993 Edition, New York, NY.

[7] Marcal, P. V., 1967, "Elastic-Plastic Behavior of Pipe Bends with In-plane Bending", *J. Strain Analysis*, Vol. 2, No. 1, pp. 84-90.

[8] Sobel, L. H., 1977, "In-Plane Bending of Elbows", *Computers & Structures*, Vol. 7, pp. 701-715.

[9] Ohstubo, H. and Watanabe, O., 1978, "Stress Analysis of Pipe Bends by Ring Elements", *J. Pressure Vessel Technology*, ASME, Vol. 100, pp. 112-122.

[10] Bathe, K.-J. and Almeida, C. A., 1980, "A Simple and Effective Pipe Elbow Element", Journal of Applied Mechanics, ASME, Vol. 47, pp. 93-100

[11] Millittelo, C. and Huespe, A. E., 1988, "A displacement-based pipe elbow element", *Computers and Structures*, Vol. 29, No.2, pp. 339-343.

[12] Yan, A. M., Jospin, R. J. and Nguyen, D. H., 1999, "An enhanced pipe elbow element – Application in plastic limit analysis of pipe structures", *International Journal For Numerical Methods in Engineering*, Vol. 46, pp. 409-431.

[13] Hibbit, H. D., Karlsson, B. I., and Sorensen, 2001, *Theory Manual*, ABAQUS, version 6.2, USA.

[14] Sobel, L. H. and Newman, S. Z., 1980, "Comparison of Experimental and Simplified Analytical Results for the In-Plane Plastic Bending and Buckling of an Elbow", *J. Pressure Vessel Technology*, ASME, Vol. 102, pp. 400-409.

[15] Sobel, L. H. and Newman, S. Z., 1986, "Simplified, Detailed and Isochronous Analysis and Test Results for the In-Plane Elastic-Plastic and Creep Behavior of an Elbow", *J. Pressure Vessel Technology*, ASME, Vol. 108, pp. 297-304.

[16] Dhalla, A. K., 1987, "Collapse Characteristics of a Thin-Walled Elbow", *J. Pressure Vessel Technology*, ASME, Vol. 109, pp. 394-401.

[17] Gresnigt, A. M. et al., 1985, "Preofresultaten van Proeven op Gladde Bochten en Vergelijking Daarvan met de in OPL 85-333 Gegeven Rekenregels", [in Dutch], *Institute for Construction Materials and Structures*, TNO-IBBC, Report OPL 85-334, Delft, The Netherlands.

[18] Hilsenkopf, P., Boneh, B. and Sollogoub, P., 1988, "Experimental Study of Behavior and Functional Capability of Ferritic Steel Elbows and Austenitic Stainless Steel Thin-Walled Elbows". *Int. J. Pressure Vessels and Piping*, Vol. 33, pp. 111-128.

[19] Suzuki, N. and Nasu, M., 1989, "Non-Linear Analysis of Welded Elbows Subjected to In-Plane bending", *Computers and Structures*, Vol. 32, No.3/4, pp. 871-881.

[20] Tan, Y., Matzen, V. C. and Yu, L., 2000, "Correlation of Test and FEA Results for the Nonlinear Behavior of Elbows", *Pressure Vessels and Piping Codes and Standards*, PVP-Vol. 407, PVP Conference, pp. 307-314.

[21] Gresnigt, A. M. and van Foeken, 1995, "Strength and Deformation Capacity of Bends in Pipelines", *International Journal of Offshore and Polar Engineering*, Vol. 5, No. 4, pp. 294-307.

[22] Gresnigt, A. M. 1986, "Plastic Design of Buried Steel Pipelines in Settlement Areas", *Heron*, Vol. 31, No. 4, Delft, The Netherlands.

[23] Shalaby, M. A. and Younan, M. Y. A., 1998, "Limit Loads for Pipe Elbows with Internal Pressure Under In-plane Closing Bending Moments", *J. Pressure Vessel Technology*, ASME, Vol. 120, pp. 35-42.

[24] Shalaby, M. A. and Younan, M. Y. A., 1999, "Effect of Internal Pressure on Elastic-Plastic Behavior of Pipe Elbows Under In-plane Opening Bending Moments", *J. Pressure Vessel Technology*, ASME, Vol. 121, pp. 400-405.

[25] Chattopadhyay J., Nathani, D. K., Dutta, B. K. and Kushwaha, H. S., 2000, "Closed-Form Collapse Moment Equations of Elbows Under Combined Internal Pressure and In-plane Bending Moment", *J. Pressure Vessel Technology*, ASME, Vol. 122, pp. 431-436.

[26] Karamanos, S. A. and Tassoulas, J. L., 1996, "Tubular Members I: Stability Analysis and Preliminary Results.", *J. Engineering Mechanics*, ASCE, Vol. 122, No. 1, pp.64-71.

[27] Karamanos, S. A. and Tassoulas, J. L., 1996, "Tubular Members II: Local Buckling and Experimental Verification.", *J. Engineering Mechanics*, ASCE, Vol. 122, No. 1, pp.72-78.

[28] Brush, D. O. and Almroth, B. O., 1975. *Buckling of Bars, Plates, and Shells*, McGraw-Hill.

[29] Giakoumatos, E., 2002, *Nonlinear Finite Element Analysis of Pipes and Elbows Under Pressure and Bending*, M.Sc. Diploma Thesis, Dept. of Mechanical & Industrial Engineering, University of Thessaly, Volos, Greece.

[30] Karamanos S. A., 2002, "Bending Instabilities of Elastic Tubes", *International Journal of Solids and Structures*, Vol. 39, No. 8, pp. 2059-2085.

[31] Karamanos, S. A. and Tassoulas, J. L., 1995, "Stability of Ring-Stiffened Tubes under External Pressure.", *J. Pressure Vessel Technology*, ASME, Vol. 117, No. 2, pp. 150-155.

[32] Donnell, L. H. and Wan, C. C., 1950, "Effects of Imperfections on Buckling of Thin Cylinders and Columns Under Axial Compression", *J. Applied Mechanics*, ASME, Vol. 17, pp. 73 – 80.

[33] Gerard, G., 1956, "Compressive and Torsional Buckling of Thin-Walled Cylinders in Yield Region", *NACA*, Technical Note 3726.

[34] Seide, P. and Weingarten V. I., 1961. "On the Buckling of Circular Cylindrical Shells Under Pure Bending.", *J. Applied Mechanics*, ASME, Vol. 28, pp. 112-116.

[35] Aksel'rad (Axelrad), E. L., 1965. "Refinement of buckling-load analysis for tube flexure by way of considering precritical deformation." [in Russian]. *Izvestiya Akademii Nauk SSSR, Otdelenie Tekhnicheskikh Nauk, Mekhanika i Mashinostroenie*, Vol. 4, pp. 133-139.

LIST OF FIGURES

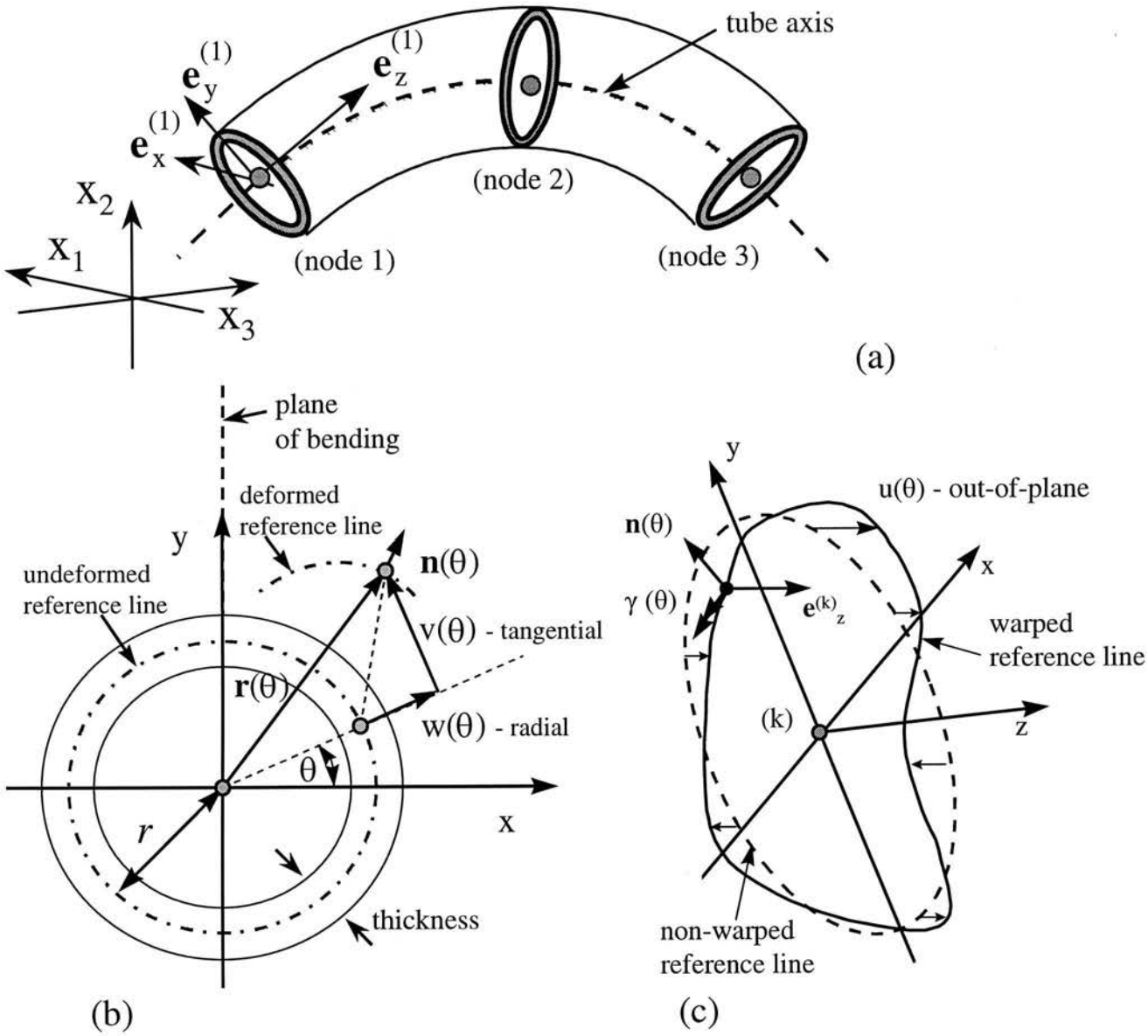

Fig. 1. Tube element; (a) general configuration, (b) in-plane deformation and (c) out-of-plane deformation.

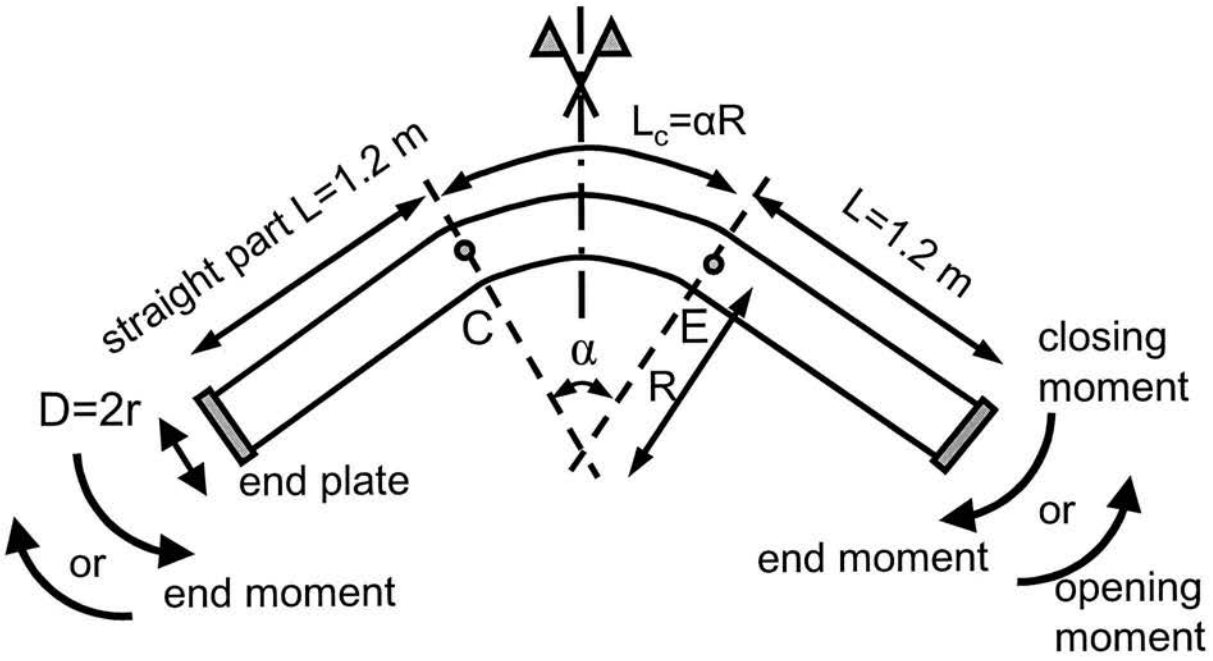

Fig. 2. TNO experiments [17]; specimen geometry.

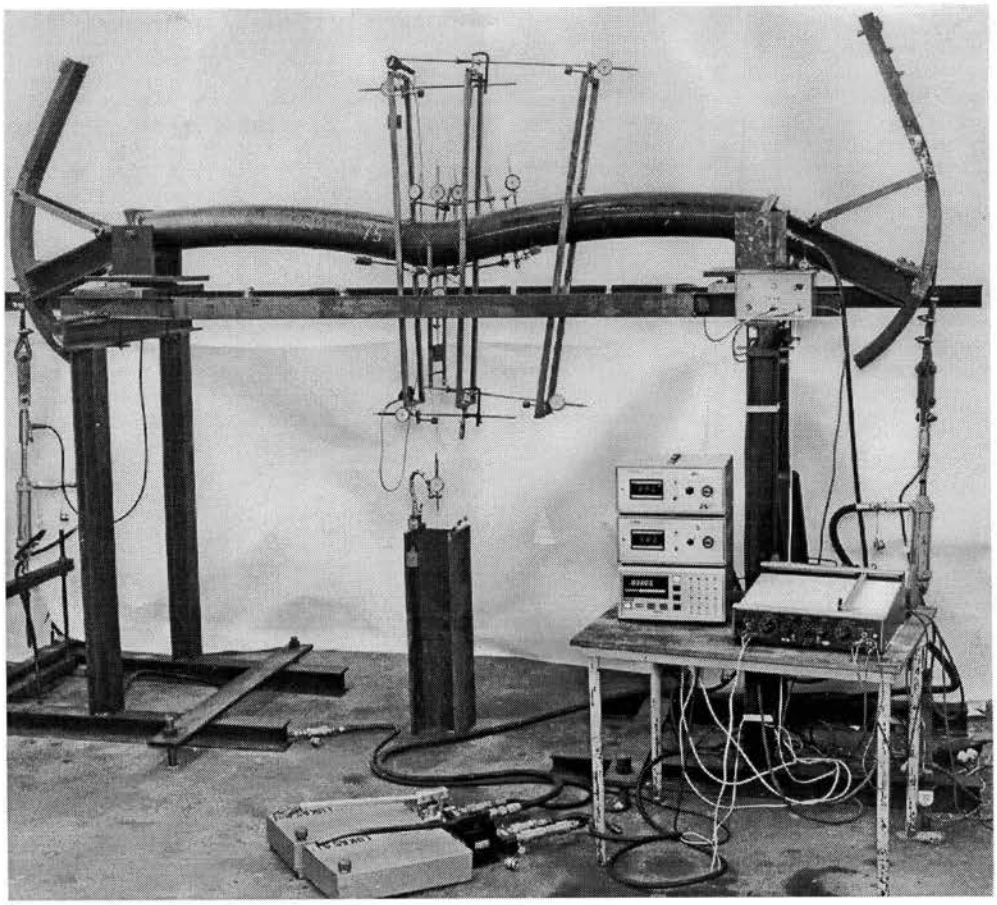

Fig. 3. Experimental set-up and final configuration of specimen 75; opening bending moments.

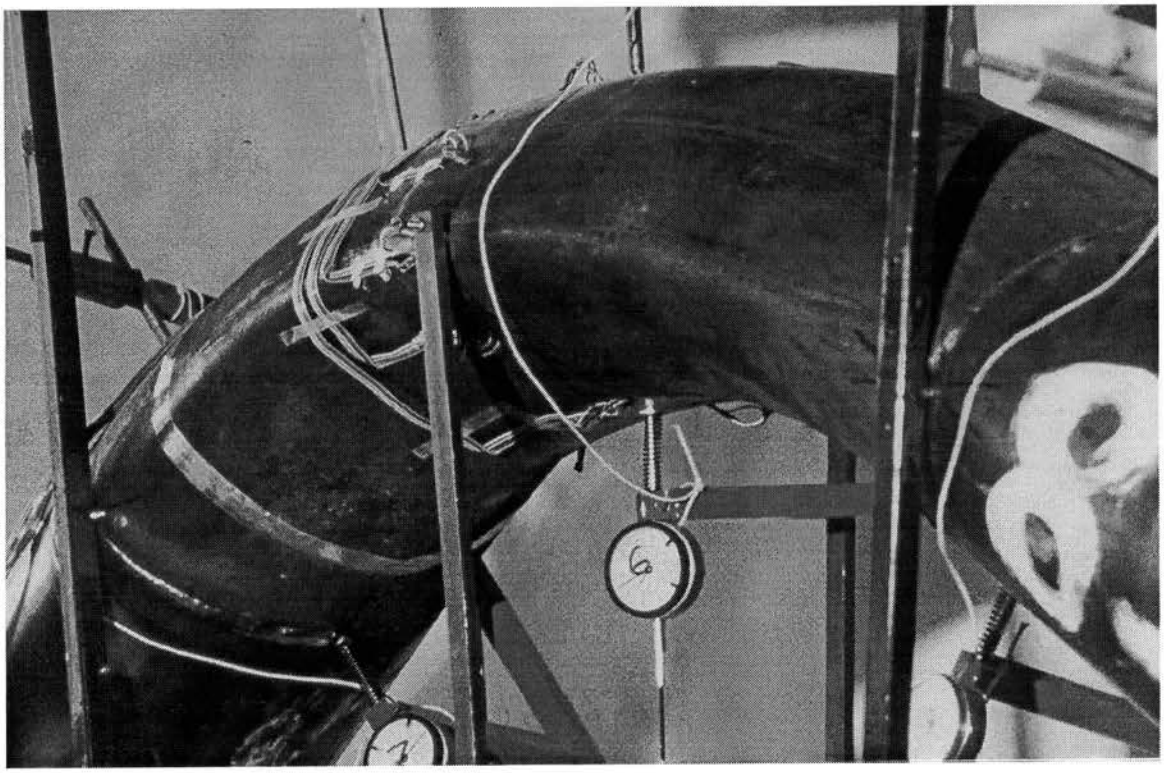

(a)

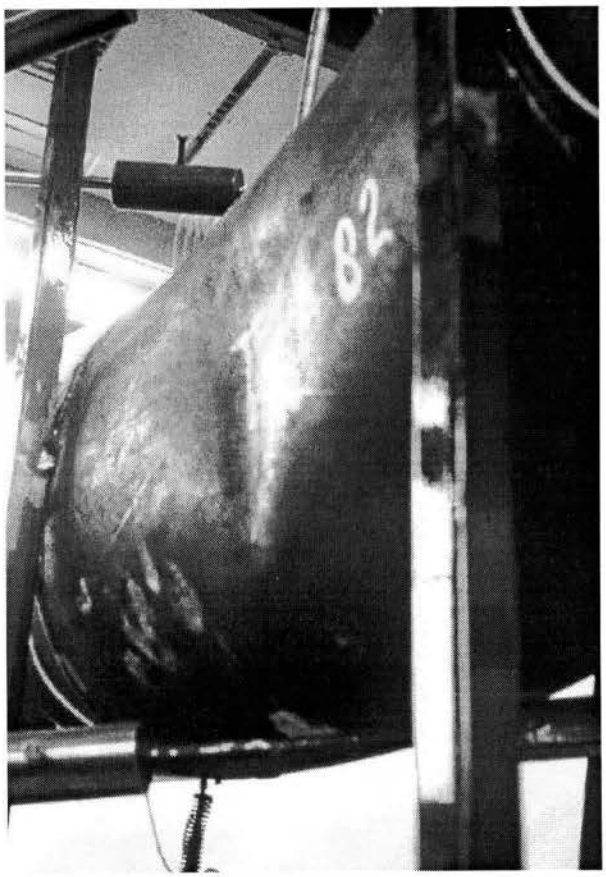

(b)

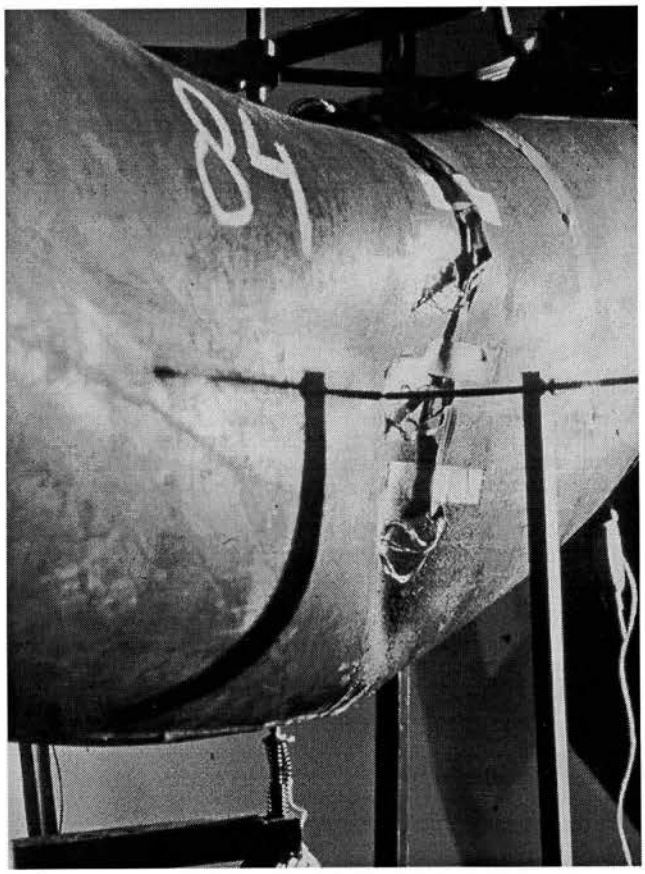

(c)

Fig. 4. (a) Flattened configuration of specimen 83 (closing moments) and (b), (c) buckled configuration of specimens 82, 84 (opening moments) - around middle cross-section of the specimen.

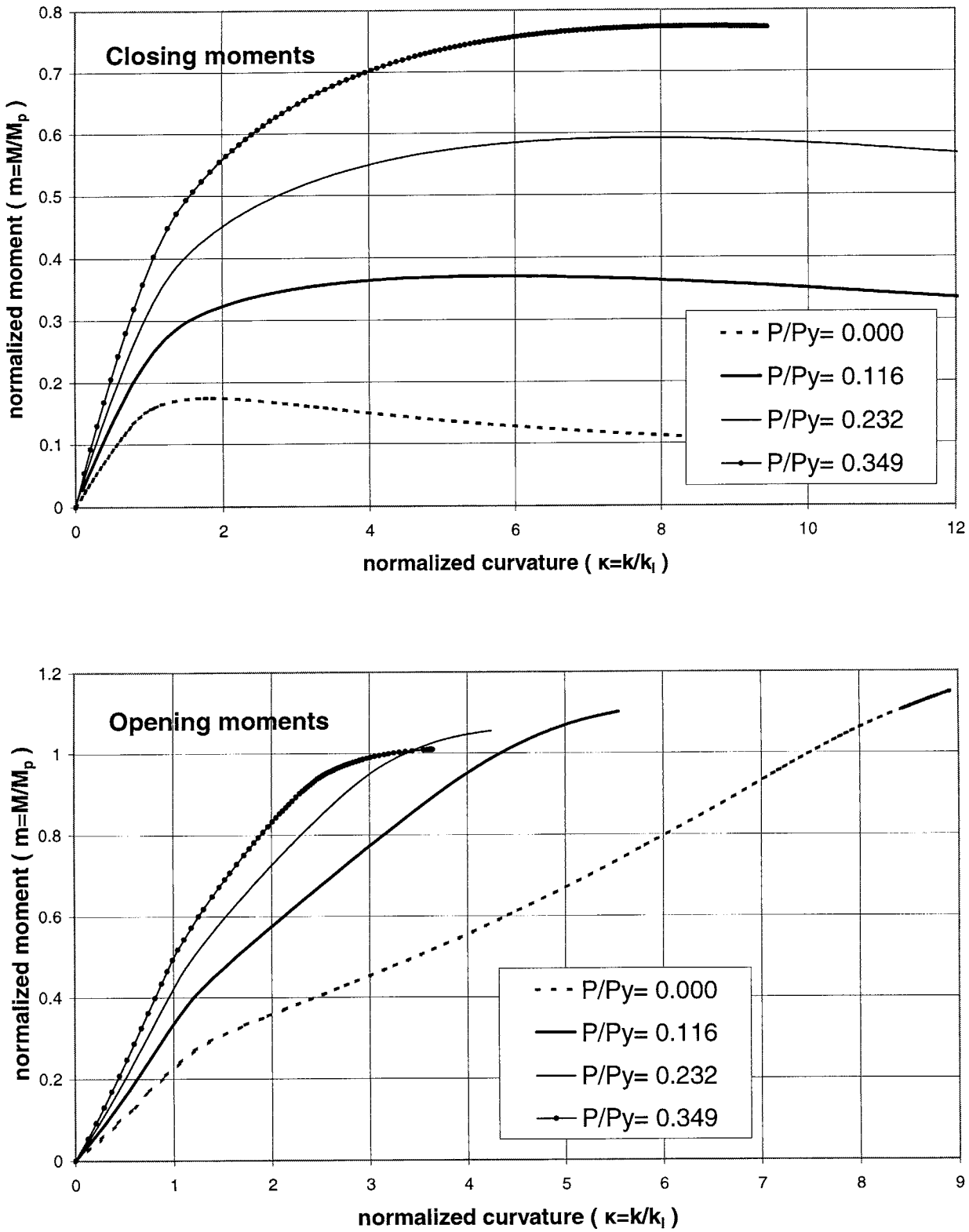

Fig. 5. Cross-sectional moment-curvature response of an elbow with D/t=90 and R/r=6 for different pressure levels; closing and opening bending moments (M_p=73,990 N-m, k_I=1.29×10^{-3} mm^{-1}, p_y=8.66 MPa); tube element analysis.

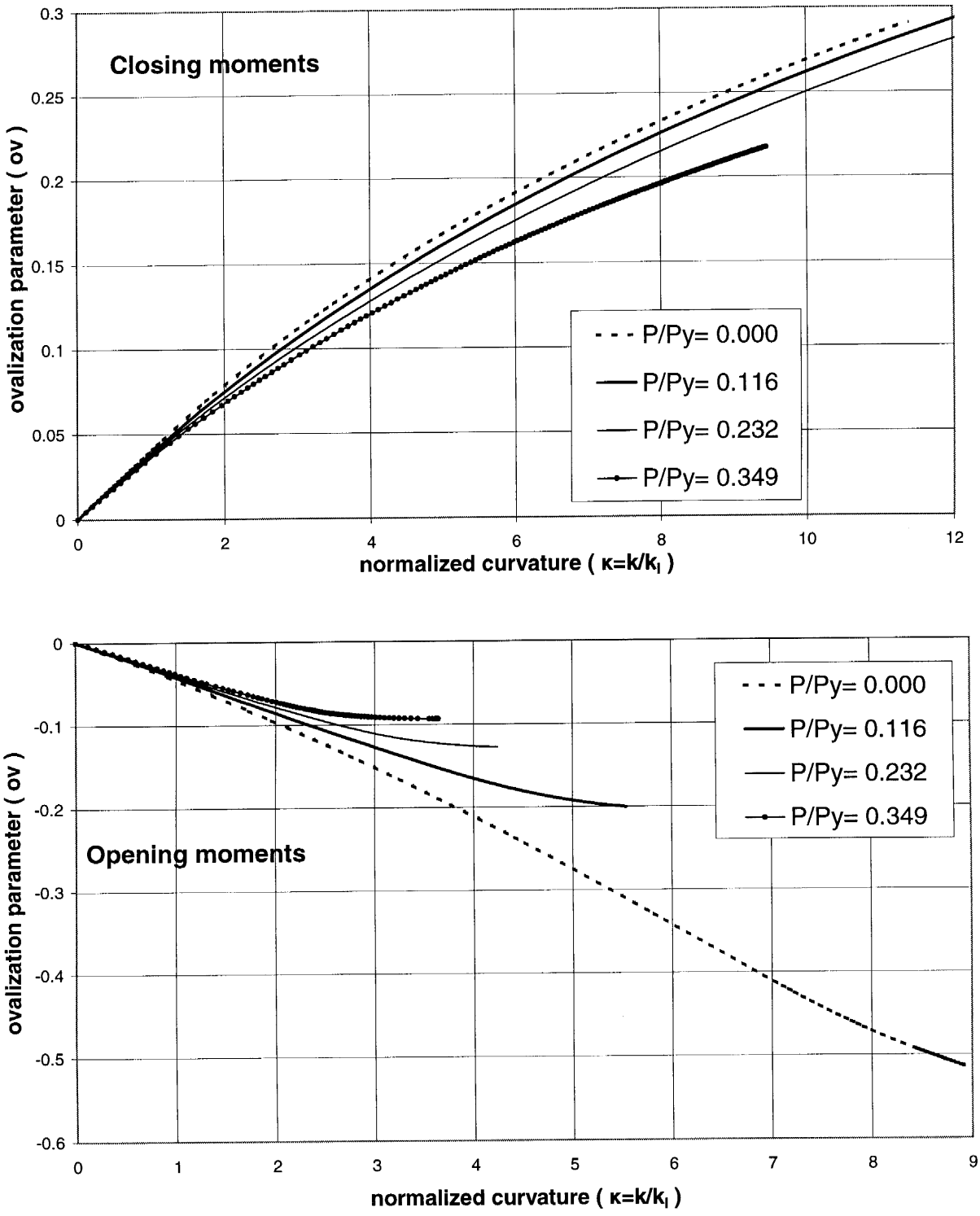

Fig. 6. Cross-sectional ovalization-curvature response of an elbow with D/t=90 and R/r=6 for different pressure levels; closing and opening bending moments (M_p=73,990 N-m, k_I=1.29×10^{-3} mm^{-1}, p_y=8.66 MPa); tube element analysis.

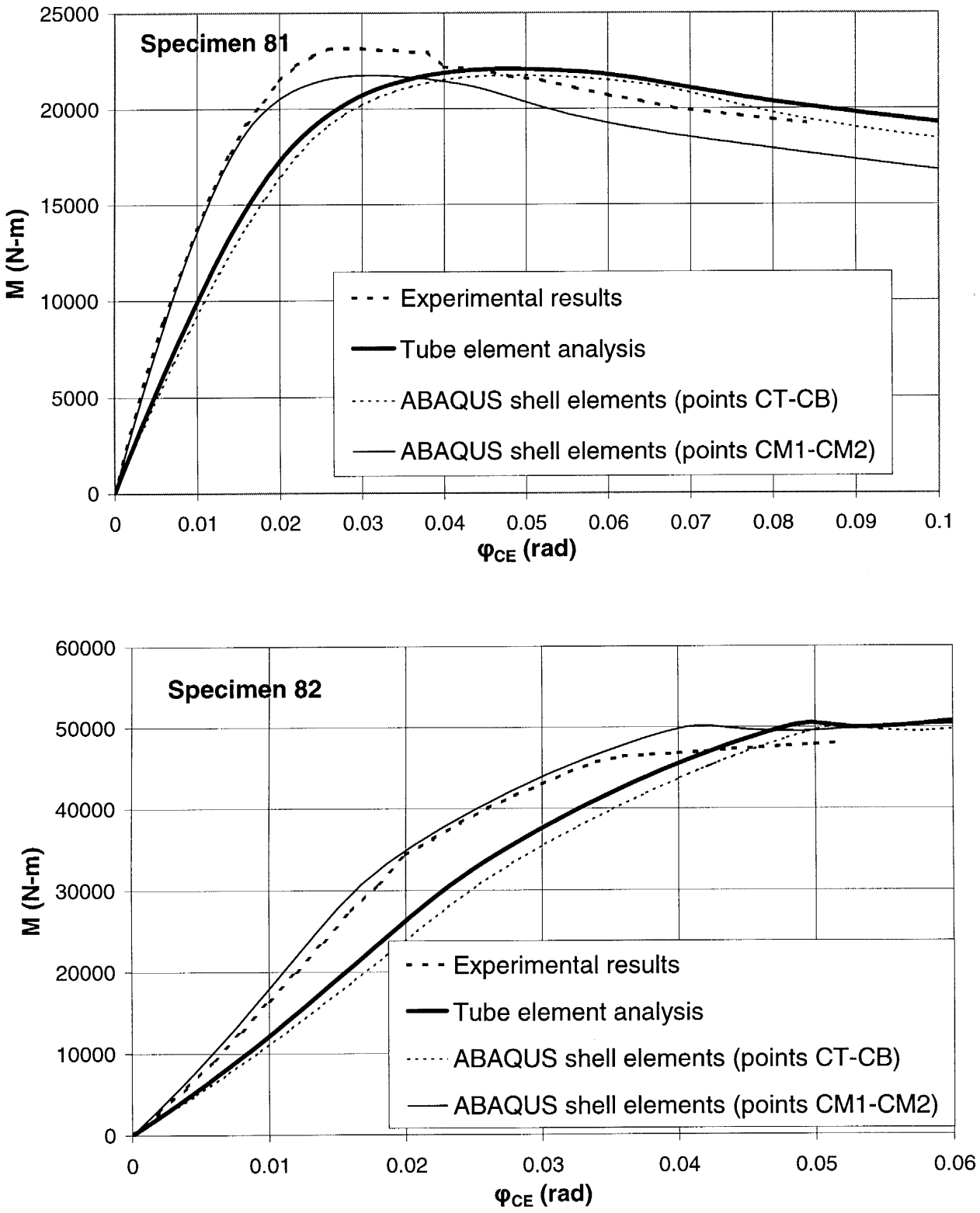

Fig. 7. Moment-rotation paths for thin non-pressurized specimens 81 and 82; comparison between test data and numerical results.

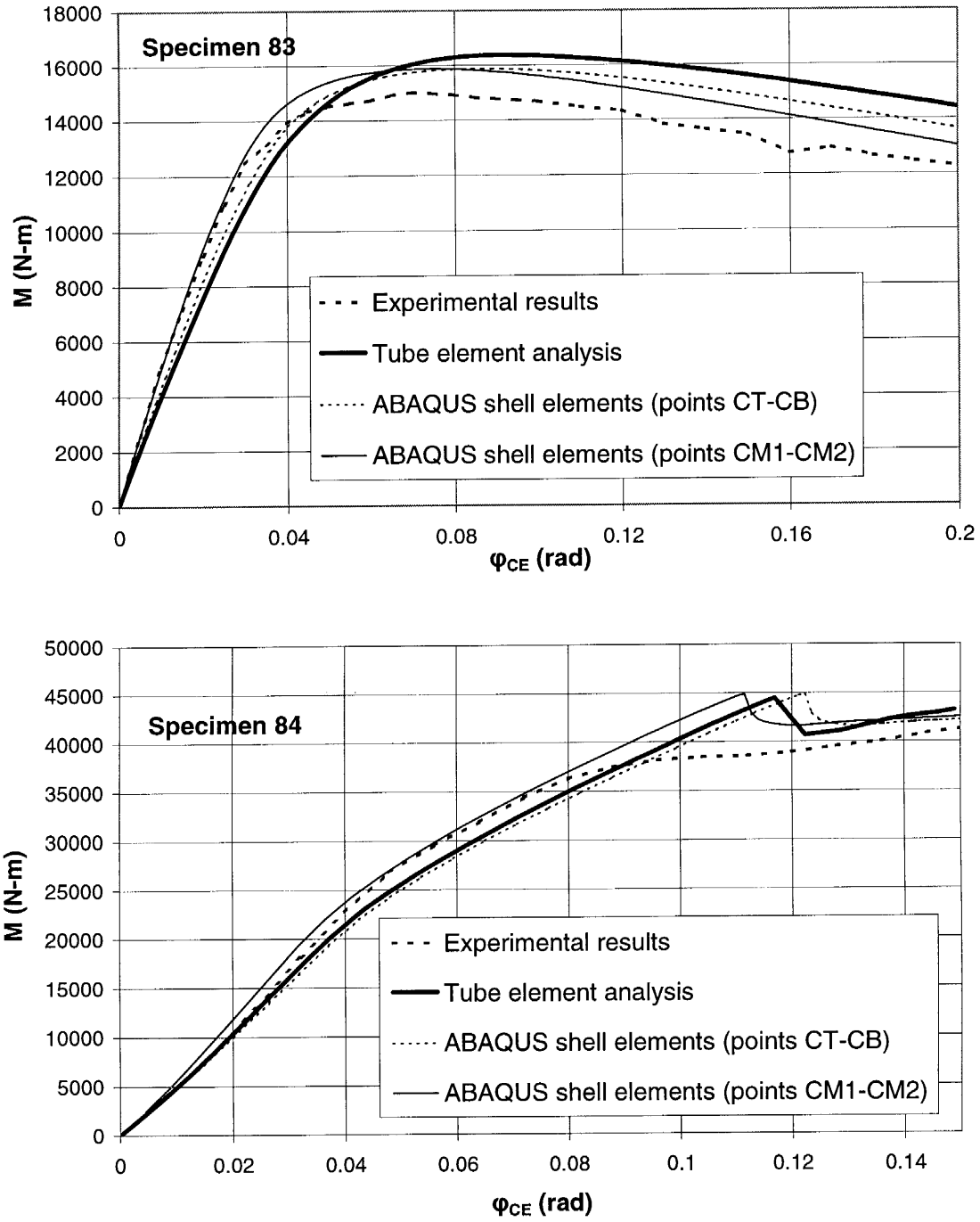

Fig. 8. Moment-rotation paths for thin non-pressurized specimens 83 and 84; comparison between test data and numerical results.

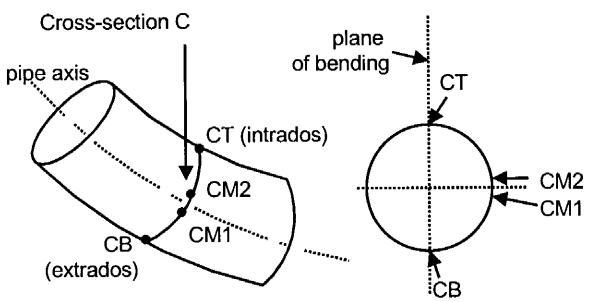

Fig. 9. Points of cross-section C employed for defining cross-sectional rotation in the course of a shell element analysis.

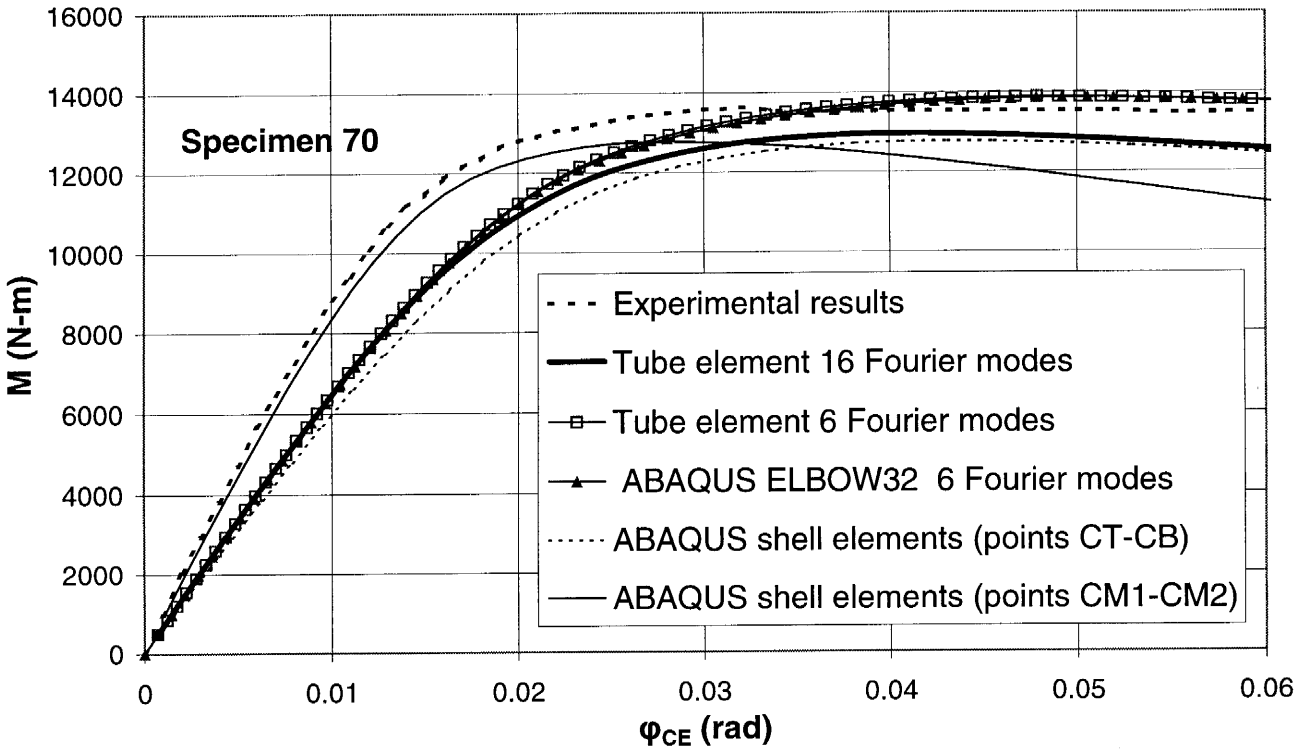

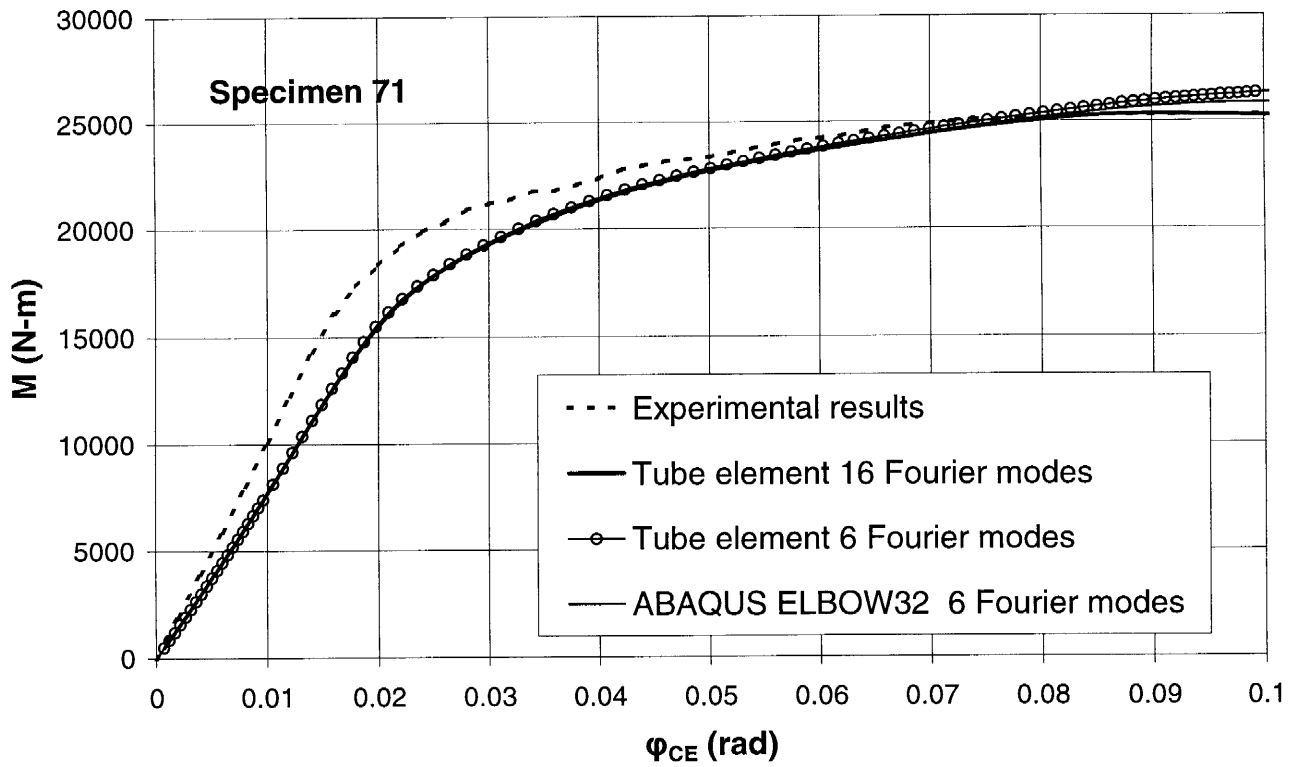

Fig. 10. Moment-rotation paths for non-pressurized specimens 70 and 71; comparison between test data and numerical results.

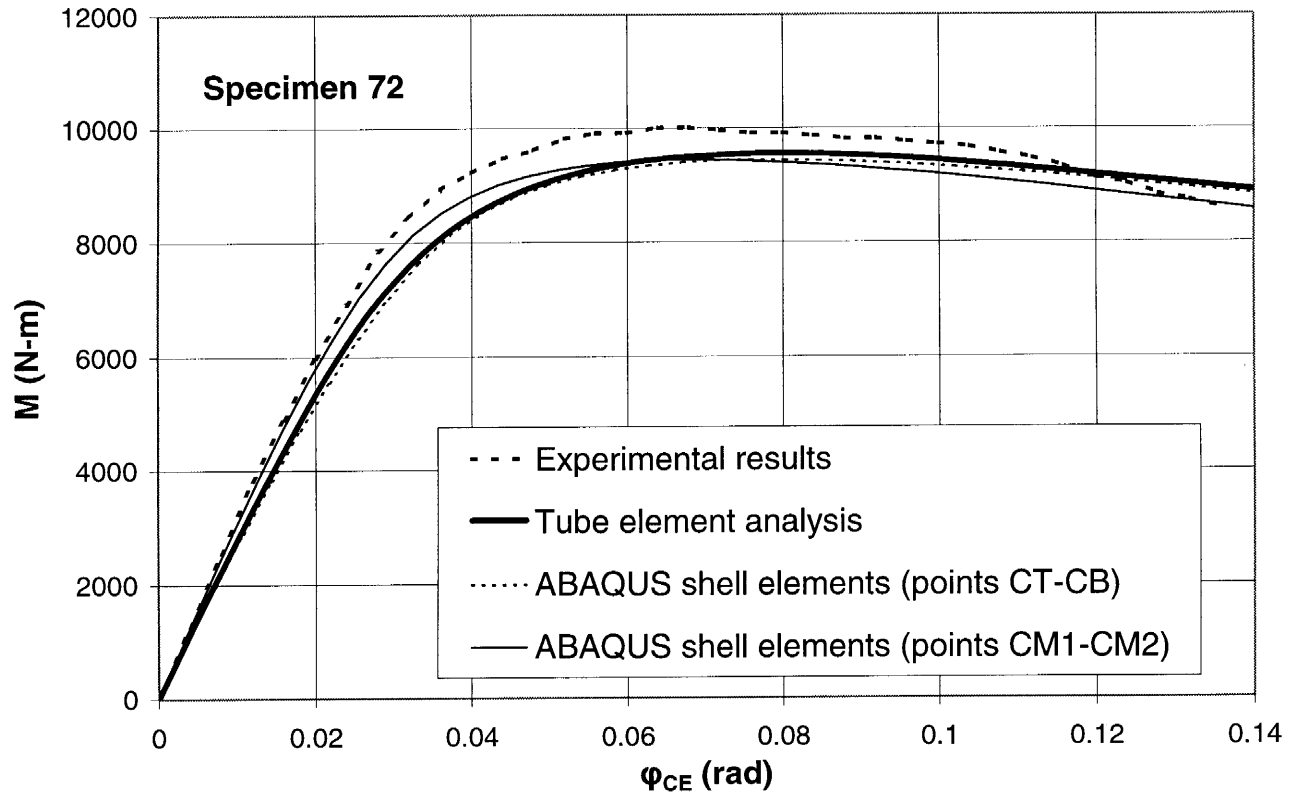

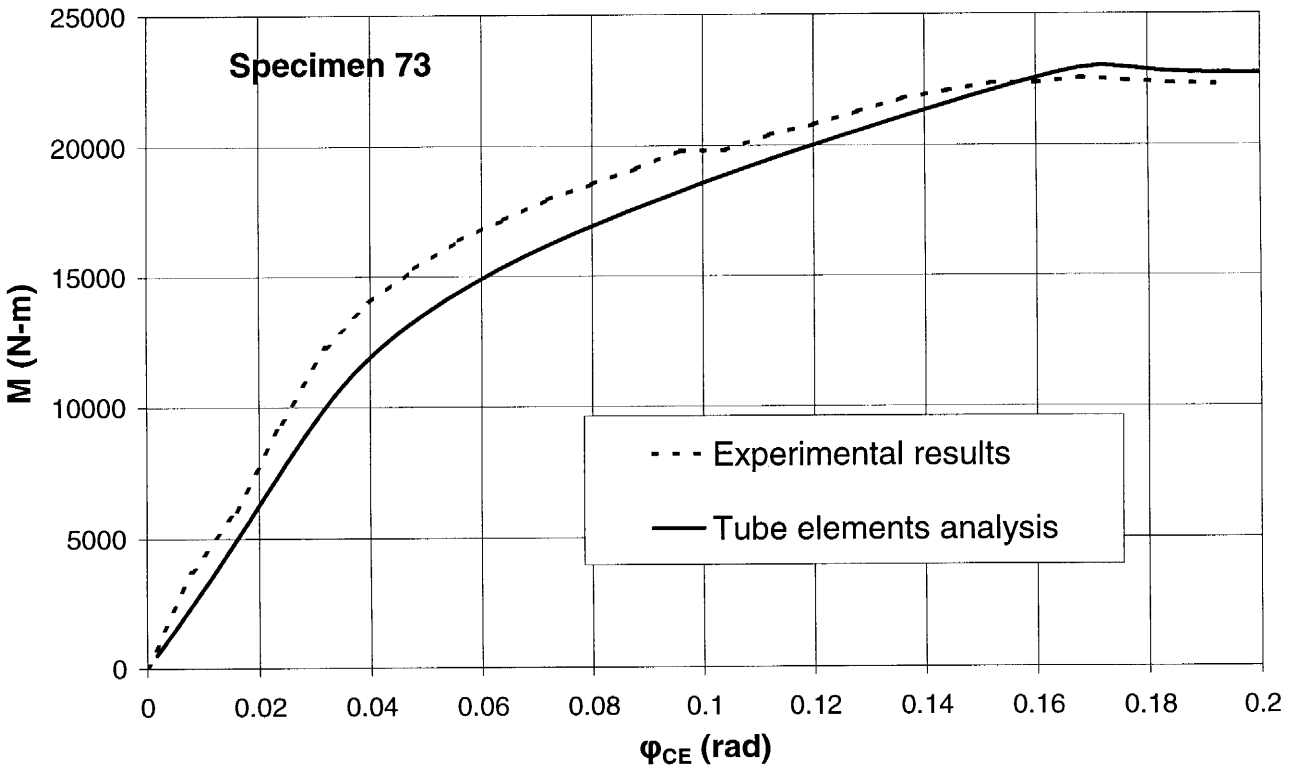

Fig. 11. Moment-rotation paths for non-pressurized specimens 72 and 73; comparison between test data and numerical results.

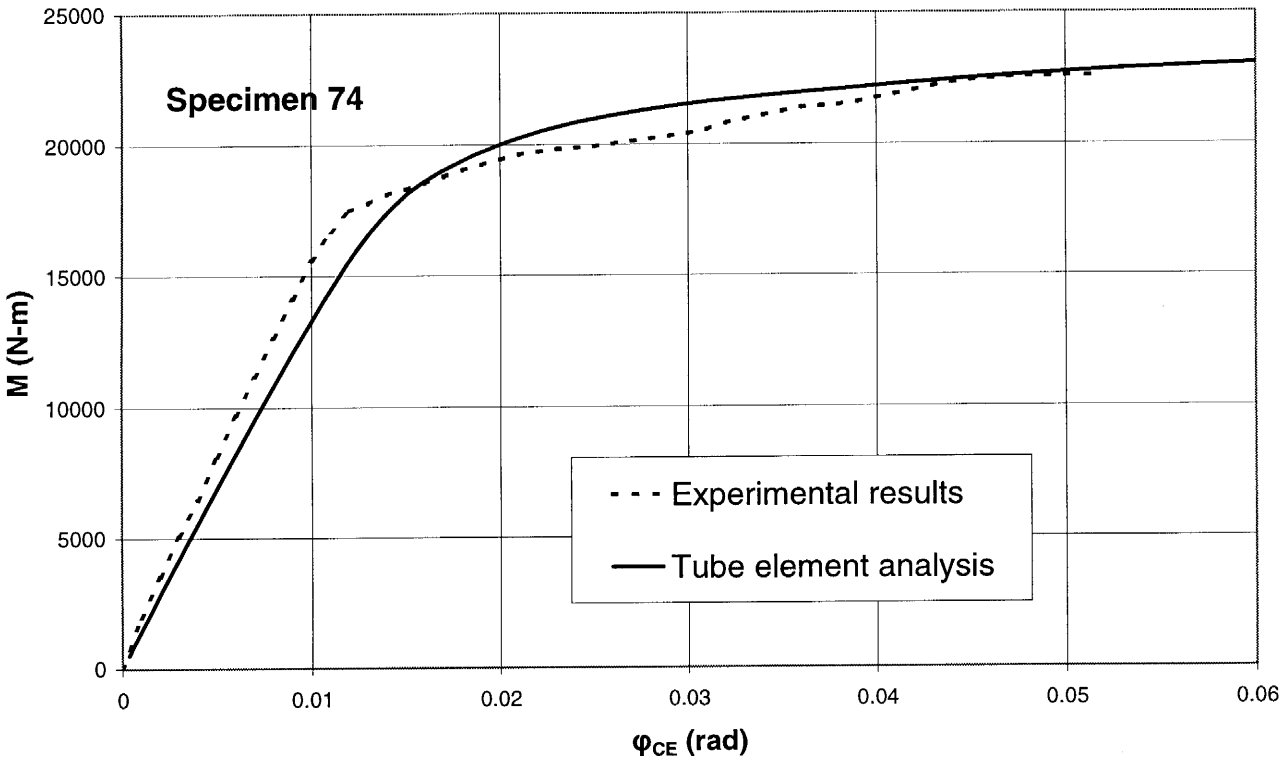

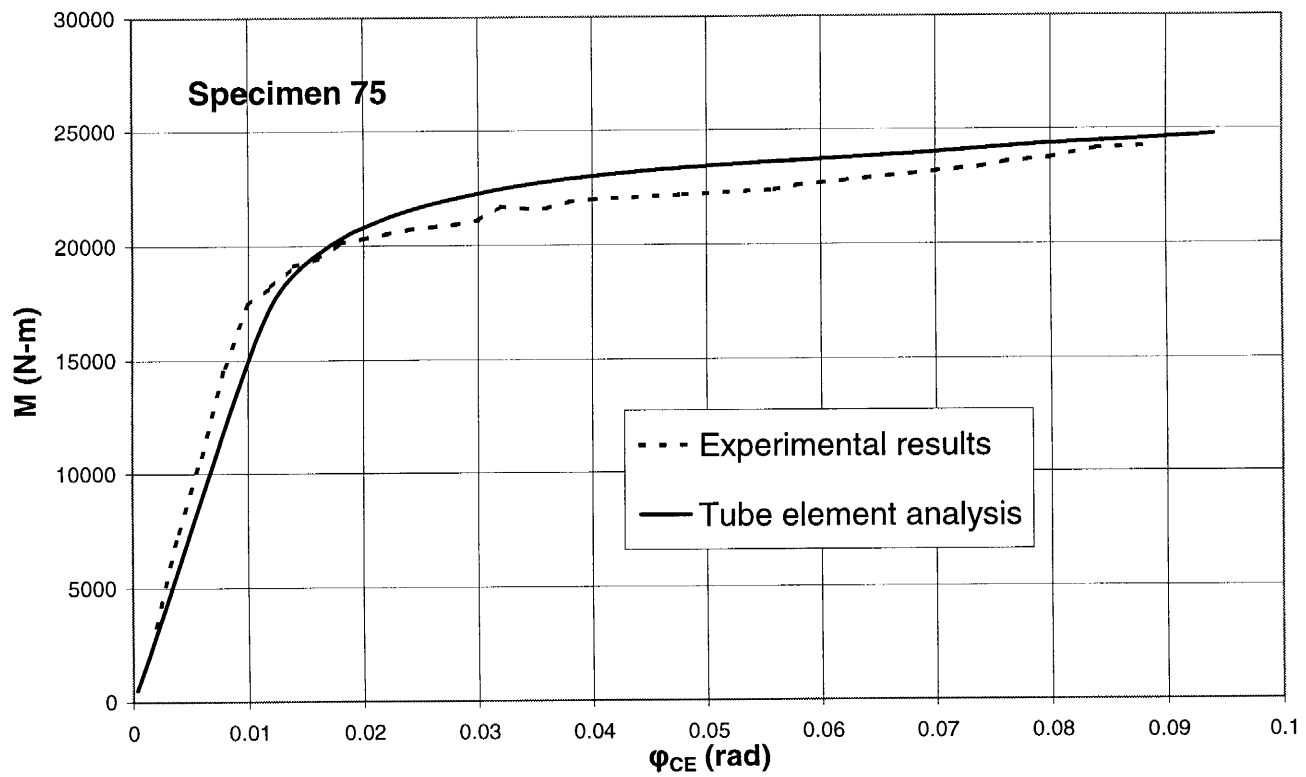

Fig. 12. Moment-rotation paths for pressurized specimens 74 and 75; comparison between test data and numerical results.

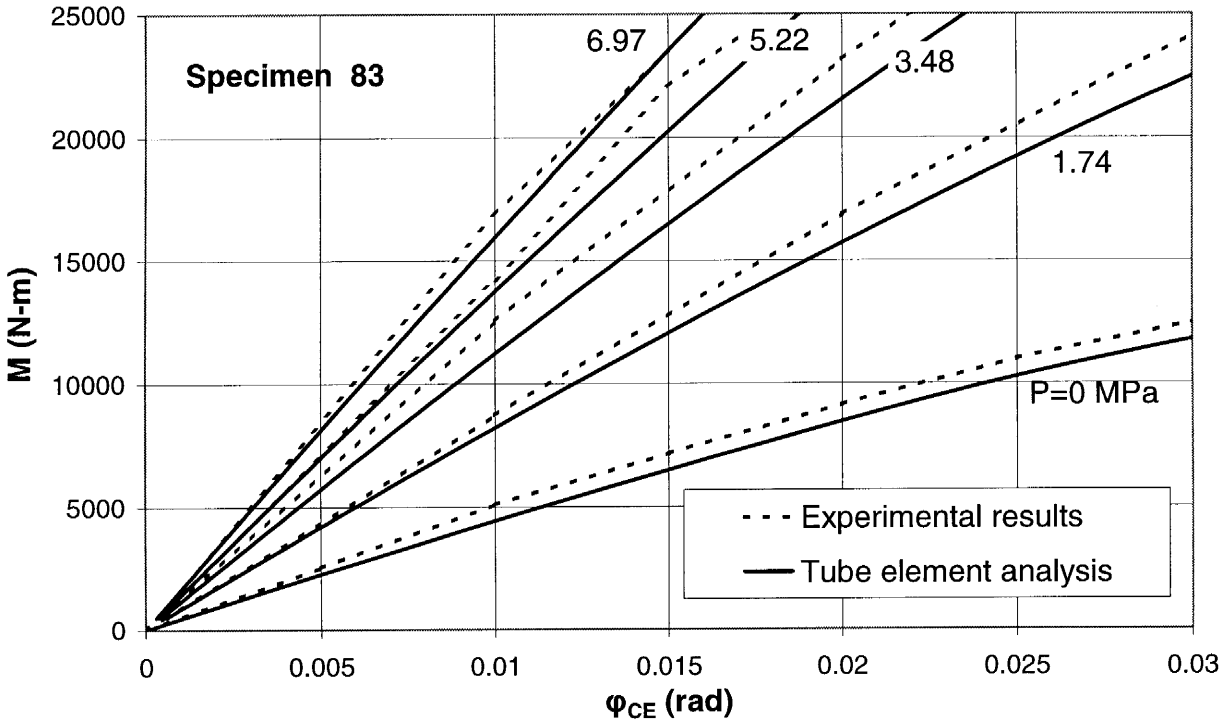

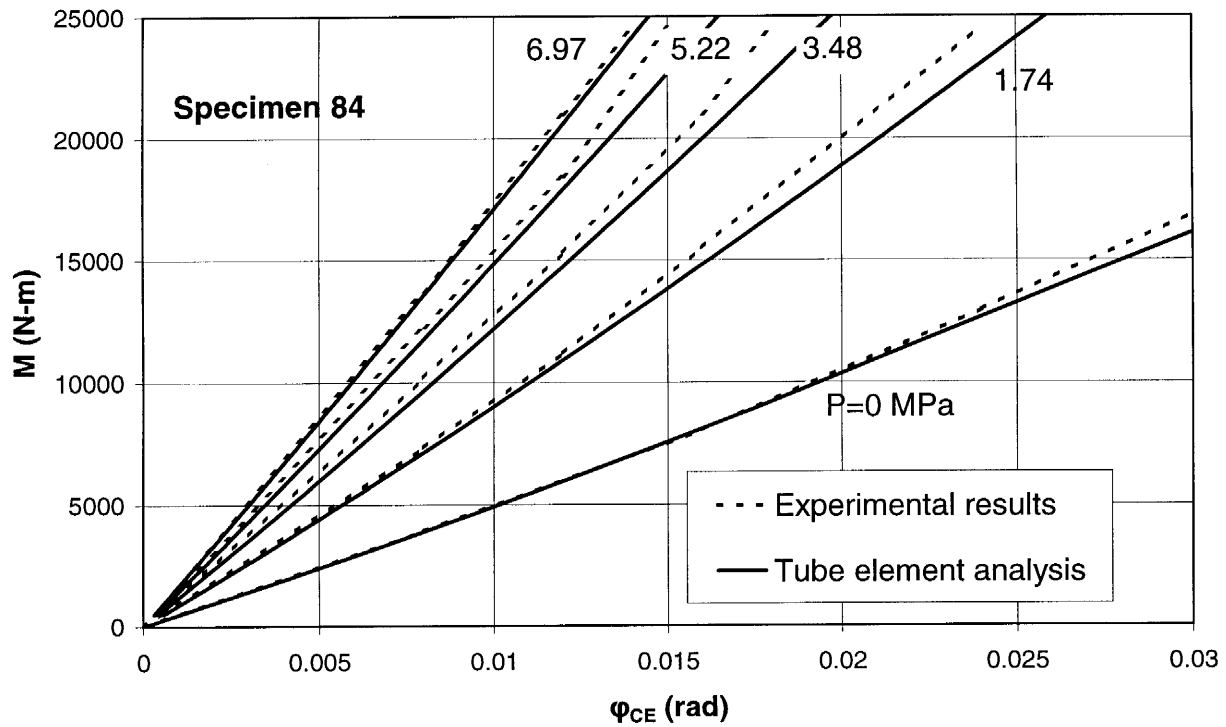

Fig. 13. Internal pressure effects on the initial flexibility of specimens 83 and 84; test data versus numerical results (pressure values in MPa).

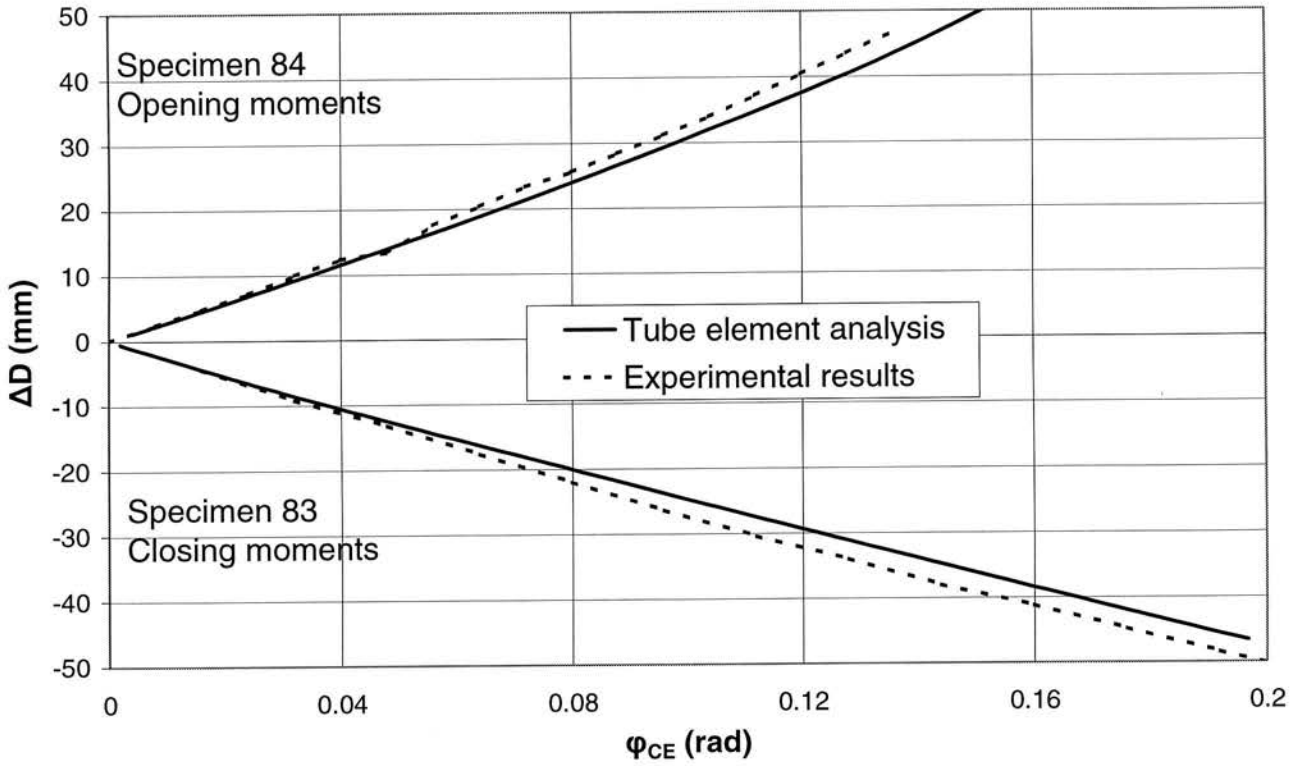

Fig. 14. Cross-sectional flattening versus rotation for moderately thin pressurized specimens 83 and 84; comparison between test data and results from tube element analysis. ΔD is the change of length of the diameter on the plane of bending.

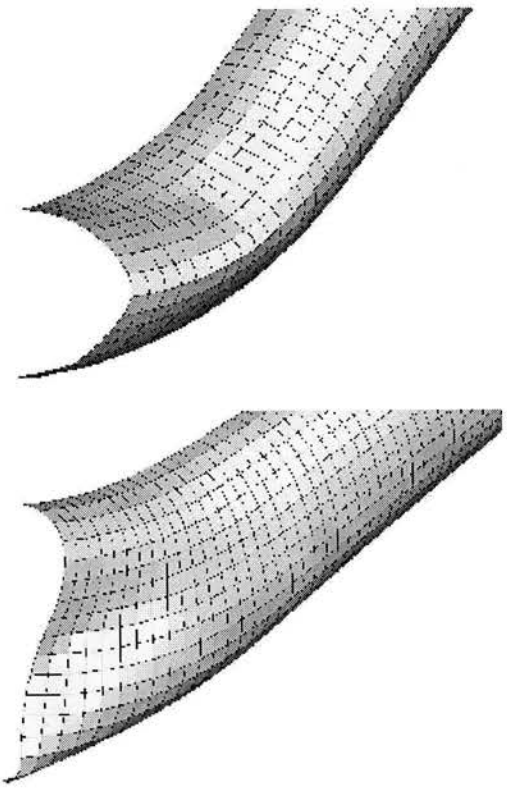

Fig. 15. (a) Ovalized shape of specimen 83 and (b) buckled shape of specimen 84 (analysis with shell element S8R5). For symmetry reasons, one-quarter of the specimens is analysed.

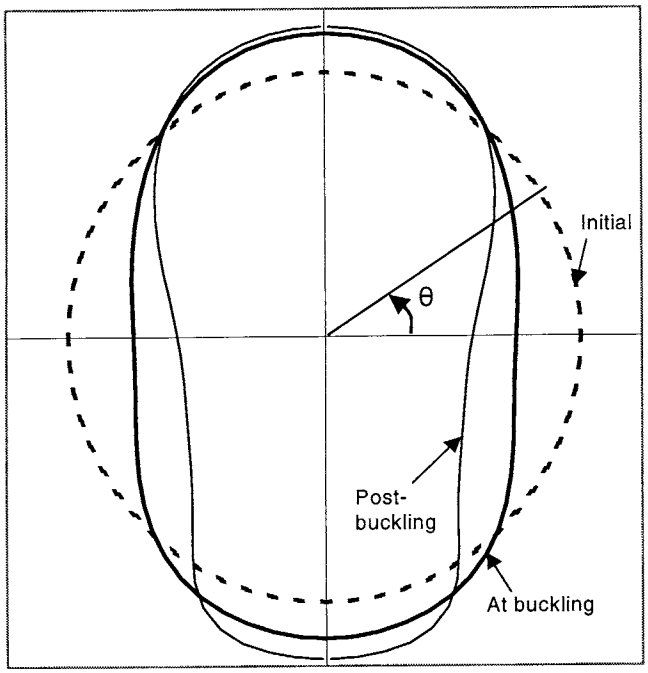

(a)

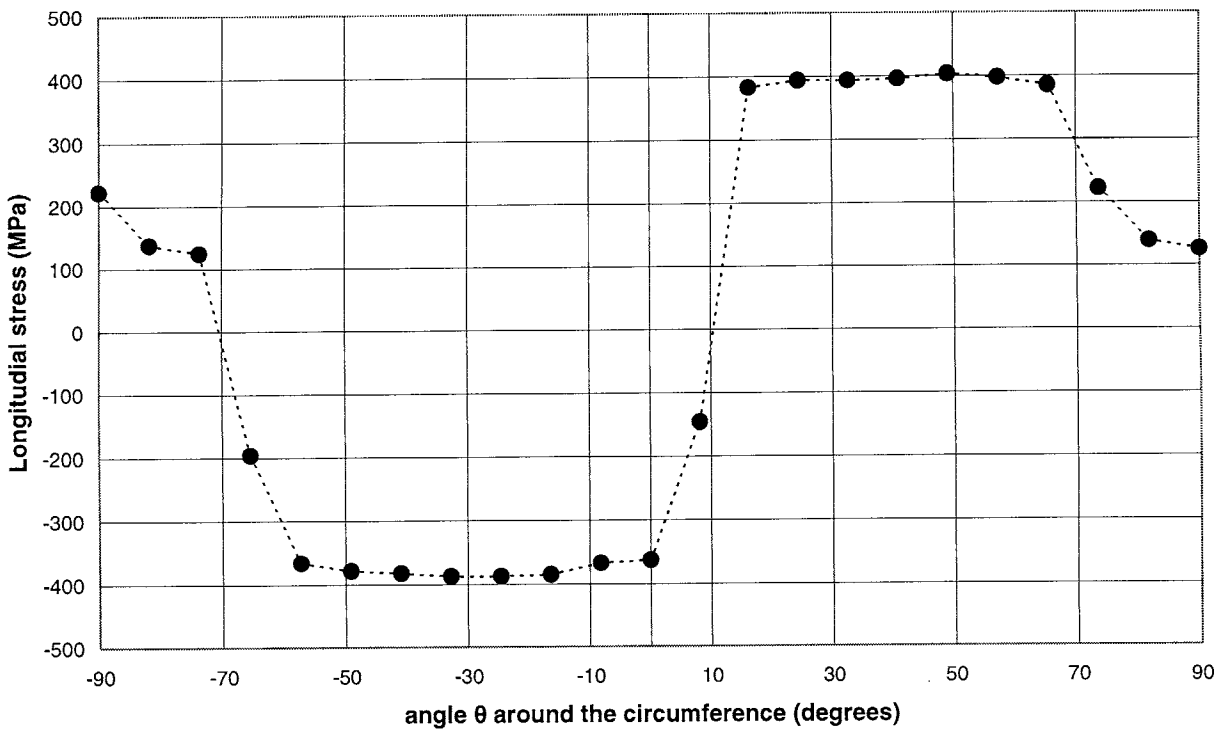

(b)

Fig. 16. (a) Deformed cross-sectional shape and (b) longitudinal stresses around the pipe middle-section of specimen 84, at buckling stage (σ_y=380 MPa).